Extrasynaptic acetylcholine signaling through a muscarinic receptor regulates cell migration

Mihoko Kato[a,1], Irina Kolotuev[b], Alexandre Cunha[c], Shahla Gharib[a], and Paul W. Sternberg[a,2]

[a]Division of Biology and Biological Engineering, California Institute of Technology, Pasadena, CA 91125; [b]Electron Microscopy Facility, University of Lausanne, Quartier Sorge-Biophore, CH-1015 Lausanne, Switzerland; and [c]Center for Advanced Methods in Biological Image Analysis, California Institute of Technology, Pasadena, CA 91125

Contributed by Paul W. Sternberg, September 6, 2020 (sent for review March 20, 2019; reviewed by Reinhard W. Köster and James B. Rand)

Acetylcholine (ACh) promotes various cell migrations in vitro, but there are few investigations into this nonsynaptic role of ACh signaling in vivo. Here we investigate the function of a muscarinic receptor on an epithelial cell migration in *Caenorhabditis elegans*. We show that the migratory gonad leader cell, the linker cell (LC), uses an M1/M3/M5-like muscarinic ACh receptor GAR-3 to receive extrasynaptic ACh signaling from cholinergic neurons for its migration. Either the loss of the GAR-3 receptor in the LC or the inhibition of ACh release from cholinergic neurons resulted in migratory path defects. The overactivation of the GAR-3 muscarinic receptor caused the LC to reverse its orientation through its downstream effectors Gαq/*egl-30*, PLCβ/*egl-8*, and TRIO/*unc-73*. This reversal response only occurred in the fourth larval stage, which corresponds to the developmental time when the GAR-3::yellow fluorescent protein receptor in the membrane relocalizes from a uniform to an asymmetric distribution. These findings suggest a role for the GAR-3 muscarinic receptor in determining the direction of LC migration.

cell migration | muscarinic receptor | acetylcholine

Acetylcholine (ACh) signaling occurs in many organs besides the nervous system, but its non-neuronal roles are less well characterized. One of the nonsynaptic functions of ACh signaling is in cell migration. Smooth muscle cells (1), epithelial keratinocytes (2), mesenchymal stem cells (3), and neuroblasts (4) all migrate in response to ACh using muscarinic ACh receptors. Additionally, ACh contributes to the metastatic migration (5) of small cell lung cancer cells (6) and cervical cancer cells (7). The muscarinic ACh receptor plays a prominent role in promoting cell migration in response to ACh. While these studies have established a connection between ACh and migration in vitro, it is less clear how ACh signaling affects various cell migrations in an organism where multiple environmental factors govern migration. In one of the few in vivo examples, ACh promotes neuronal migration in zebrafish (8).

The linker cell (LC) is a migratory epithelial cell located at the front of the developing male gonad of *C. elegans*. Previously through single-cell transcriptional profiling, we unexpectedly found that the LC expresses neuronal receptors (9), one of which was the muscarinic ACh receptor GAR-3. The LC leads a complex but stereotypic migration that is followed by interconnected gonadal cells during the second to fourth larval (L2 to L4) stages (Fig. 1 *A* and *B*). Through this migration, the LC guides the developing gonad to the cloaca opening, and in the process, generates the shape of the adult gonad. Both the profiling results and a transcriptional yellow fluorescent protein (YFP) reporter showed that the LC expresses *gar-3* during its L3 and L4 stage migrations. GAR-3 is functionally most similar to the M1/M3/M5 muscarinic receptors in humans, which are Gαq-coupled receptors (10). GAR-3 function has been studied in excitable cells of *C. elegans*, such as certain neurons and muscle (11–14), but its role in nonexcitatory cells is unknown.

Given the involvement of muscarinic receptors in the migration of normal (1–4) and cancer cells (15, 16), we decided to investigate GAR-3's function in LC migration. We found that *gar-3* loss of function (lf) caused the LC to stray from its normal migratory path. The overactivation of the GAR-3 receptor resulted in the LC reversing its orientation. Downstream of *gar-3*, the LC used both *egl-8*/PLCβ and *unc-73*/TRIO branches of the *egl-30*/Gαq pathway. We determined that the LC likely receives ACh from the VNCs and DNCs, which run parallel to the LC's migratory course. Reduction of ACh release through mutants in cholinergic neuron function resulted in similar defects as *gar-3* mutants. We propose that the LC uses the GAR-3 receptor to sense extrasynaptic ACh that is released from the nerve cords in order to refine its direction of migration.

Results

***gar-3* Functions in Refining the LC Migratory Course.** We investigated whether *gar-3* lf affects LC migration. In 23% ($n = 73$) of *gar-3* deletion mutants, the gonad had an abnormal shape that indicated a defect in the LC migratory path (Fig. 1*C*). The most common defect was that the LC had a migratory defect in the L3 stage that resulted in the dorsal to ventral turn occurring at a later point in its migration rather than its normal position, which occurs immediately after reaching the distal end of the gonad (Fig. 1 *C* and *D*). The migratory defects led to a sloppy execution of its normal migration but did not affect the ability of the LC to reach the cloaca at the end at its normal time.

Neuronally Released ACh Is Used for LC Migration. Considering the trajectory of LC migration, the closest sources of ACh are

Significance

Although ACh is best known for its role in neurotransmission, it also plays a role in cell migration. ACh promotes various cell migrations in vitro, but little is known how it affects cell migration inside an organism where multiple environmental cues are involved. We investigated the migration of an epithelial cell in *C. elegans*, the gonad leader cell, which expresses a muscarinic acetylcholine receptor. This leader cell migrates closely along the animal's nerve cords and uses ACh secreted from cholinergic neurons. The muscarinic receptor helps the leader cell stay on its migratory path, but its overactivation causes a reversal in cell orientation. The leader cell may use the muscarinic receptor to adjust its orientation to stay on its migratory path.

Author contributions: M.K., I.K., and P.W.S. designed research; M.K., I.K., and S.G. performed research; M.K. and A.C. contributed new reagents/analytic tools; M.K., I.K., and A.C. analyzed data; and M.K. and P.W.S. wrote the paper.

Reviewers: R.W.K., Technische Universität Braunschweig; and J.B.R., University of Oklahoma Health Sciences Center.

The authors declare no competing interest.

[1]Present address: Biology Department, Pomona College, Claremont, CA 91711.

[2]To whom correspondence may be addressed. Email: pws@caltech.edu.

This article contains supporting information online at https://www.pnas.org/lookup/suppl/doi:10.1073/pnas.1904338118/-/DCSupplemental.

Published December 23, 2020.

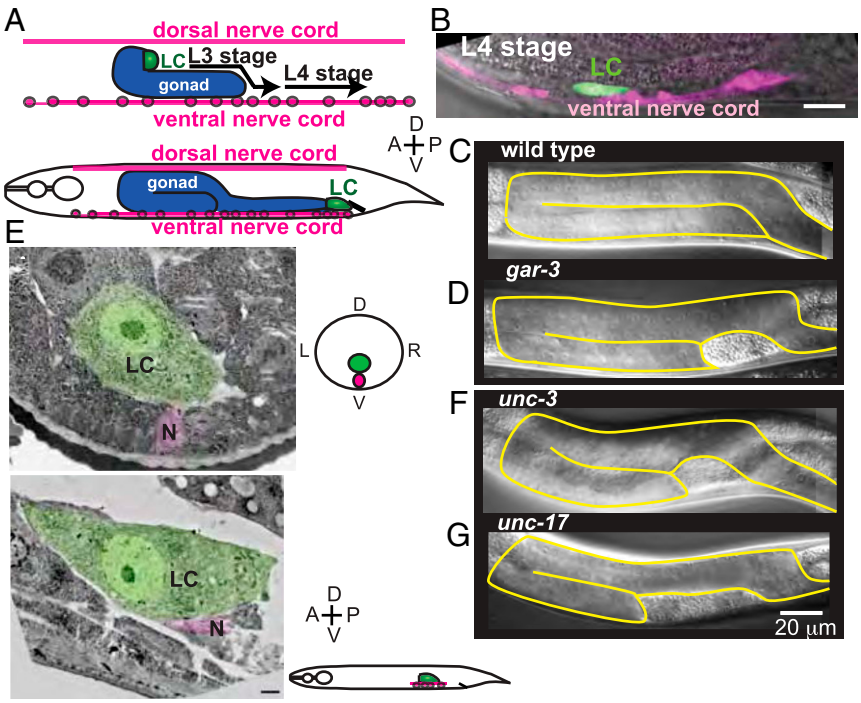

Fig. 1. The LC migrates along the nerve cords using ACh signaling. (*A*, *Top*) The gonad at the beginning of the third larval (L3) stage. The arrows depict the LC migratory path during the L3 and fourth larval (L4) stages, which occurs along the dorsal nerve core (DNC) and ventral nerve cord (VNC). The shape of the gonad is determined by the migratory path of the LC. (*Bottom*) The resulting gonad at the end of the L4 stage. (*B*) overlay of a confocal image of the LC (green) and VNC (pink) and a differential interference contrast image of the L4 stage animal. (Scale bar is 10 μm.) (*C*, *D*, *F*, *G*) L4 stage gonads of (*C*) a wild-type animal, (*D*) *gar-3* deletion mutant, (*F*) *unc-3(lf)* mutant, (*G*) and *unc-17(lf)* mutant. (*E*) Electron micrograph (EM) of LC (green) and VNC neuron (*Top*) or neurites (*Bottom*) in a transverse cross section (*Left*) and longitudinal cross section (*Right*).

cholinergic neurons of the VNC and their neurites in the DNC (Fig. 1 *A* and *B*). The VNC consists of a row of neuron cell bodies and neurites while the DNC consists only of neurite projections from the cells in the VNC. The LC migrates along the DNC during most of the L3 stage, and along the VNC from the late L3 stage, and throughout the L4 stage. By examining the LC using EM, we determined that the LC gets as close as several nanometers to the ventral neuron cell bodies and neuronal processes (Fig. 1*E* and *SI Appendix*, Fig. S1). While the distance is close enough for contact, we did not observe any evidence of direct contact.

We hypothesized that extrasynaptic ACh from cholinergic neurons may diffuse to the LC and be used for its migration. To determine if *gar-3* signaling in the LC is dependent on ACh signaling from cholinergic neurons, we examined the effect of cholinergic neuronal mutants on LC migration. The *unc-3* mutant (42% abnormal, $n = 33$), which lacks a transcription factor required for specification of cholinergic fate for most cholinergic neurons in the VNC (17, 18) and the *unc-17* mutant (20% abnormal, $n = 20$), which lacks the synaptic vesicle ACh transporter (19), have defects in LC migratory path similar to the *gar-3* mutant, particularly, in the dorsal to ventral turn (Fig. 1 *C*, *D*, and *F*). These data indicate that cholinergic neurons are likely the source of ACh for the LC. To test whether the LC migration defect observed in cholinergic signaling mutants is an indirect consequence of an early developmental defect in cholinergic neurons or in ACh release alone, we knocked down *unc-3* postembryonically in the L1 stage using an inducible degron system (20, 21). Animals expressing a modified *Arabidopsis* TIR1 F-box protein and *unc-3::mNeonGreen::AID*, which has the endogenous *unc-3* locus tagged with a fluorescent protein and auxin-inducible degron, were treated with 1 mM auxin in the mid-L1 and scored for male gonad defects in the L4 stage. Some 9.7% ($n = 72$) of *unc-3* degron-tagged animals, compared to 5.8% ($n = 51$) of wild-type animals, showed LC migratory path defects. This suggests that the LC migratory defects resulting from *unc-3* mutants are caused not only by the lack of ACh signaling during cell migration, but also mainly by other functions of *unc-3* and, therefore, cholinergic neurons before the onset of migration. None of the *unc-3::mNeonGreen::AID* animals had any detectable fluorescence at the time of scoring in the L4 stage, indicating that *unc-3* had, in fact, been degraded. In a smaller test case, we saw no fluorescence 1 h after starting auxin treatment. Previous studies have shown that continued *unc-3* expression is required to maintain cholinergic identity (18). The LC defects in the *unc-3* mutant may be the result of confounding factors that include embryonic cholinergic development. The LC typically completed the migration in *gar-3*, *unc-3*, and *unc-17* mutants, suggesting that ACh signaling is not necessary for LC migration but is instead used to refine it.

Overactivation of the GAR-3 Receptor Leads to Reversal of Cell Orientation. We next examined the effect of GAR-3 overactivation on LC migration. We increased the concentration of extracellular ACh by using aldicarb, an acetylcholinesterase inhibitor, which promotes the accumulation of ACh at sites of release. Treating animals with aldicarb unexpectedly resulted in a new phenotype of the LC reversing its orientation under certain conditions. LC orientation and migratory direction can be determined by its polarized morphology in which the nucleus is always positioned in the lagging end of an elongated cell (Fig. 2 *A* and *B*). EM confirmed that the nucleus occupies the lagging end of the cytoplasm while revealing that organelles, such as the mitochondria, are located in the leading end (Fig. 2*B* and *SI Appendix*, Fig. S2). Since the LC migrates toward the posterior end of the body during the L3 and L4 stages, the LC in untreated animals faced

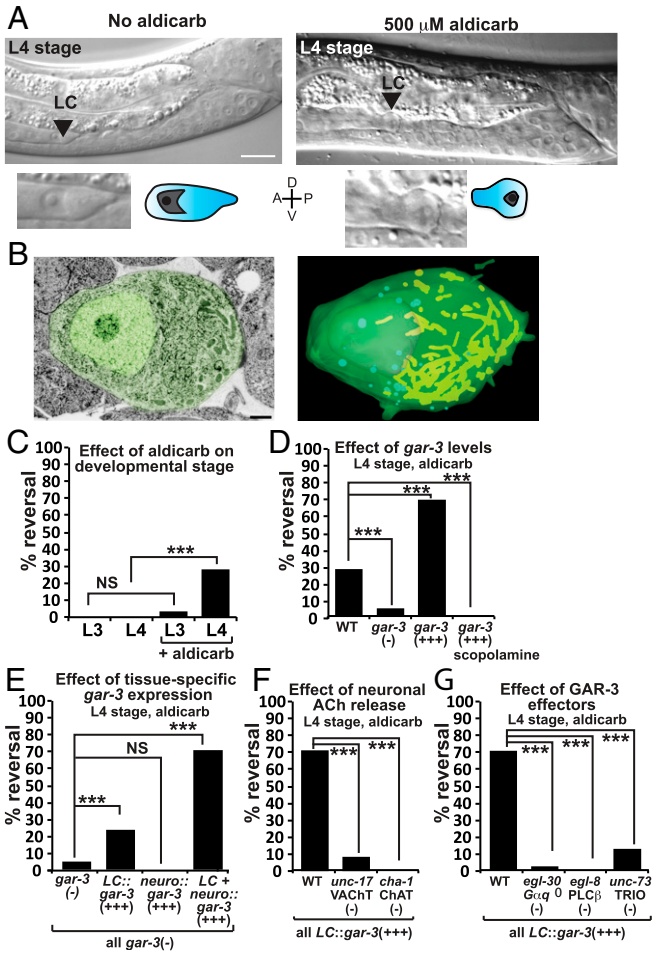

Fig. 2. Aldicarb treatment causes LC reversals under certain conditions. (*A*) Nomarski images of the L4 stage LC. (*Left*) In the posteriorly migrating LC, the nucleus is located at the lagging end of the cell. (*Right*) In an animal treated with 500 μM aldicarb, the LC has reversed its orientation to face the anterior direction as indicated by the nucleus in the posterior position. (Scale bar: 10 μm.) (*B*) An EM of the LC (*Left*) and the three-dimensional reconstruction of the mitochondria (yellow) in the LC show that the mitochondria are in front of the nucleus. (Scale bar: 1 μm.) (*C*) The percentage of LCs with reversed orientation in the L3 (n = 30) and L4 (n = 34) stages of control animals and in the L3 (n = 32) and L4 (n = 64) stages with 500 μm aldicarb treatment. (*D*) The percentage of LC reversals with levels of *gar-3* expression that are wild type (n = 64), no expression (n = 69), overexpression in the LC (n = 86), and overexpression in the LC plus scopolamine, a *gar-3* selective antagonist (n = 33). (*E*) The percentage of LC reversals when *gar-3* mutants were rescued with LC expression of *gar-3* (n = 65), VNC expression of *gar-3* (n = 9) or both (n = 27). (*F*) The percentage of LC reversals in *unc-17* (n = 12) and *cha-1* (n = 12) mutants, defective in ACh release from cholinergic neurons. (*G*) The percentage of LC reversals in mutants of the *gar-3* downstream effectors *egl-30*/Gαq (n = 39), *egl-8*/PLCβ (n = 25), and *unc-73*/TRIO (n = 24). Statistical significance was calculated using Fisher's exact test. $P < 0.0001$ is statistically significant and denoted by ***. N.S., not significant.

the posterior direction as expected (L3 stage 0% reversal, n = 30; L4 stage 0% reversal, n = 34). Treating animals with 500 μM aldicarb to increase extrasynaptic ACh levels resulted in the LC reversing its orientation from the posterior to the anterior direction in a stage-dependent manner. While aldicarb-treated L3 stage males showed almost no LC reversals (3.4% reversal, n = 32), 28% (n = 64) of L4 stage males had anterior-facing reversed LCs (Fig. 2*C*). We tested whether the LC reversal in the L4 stage is dependent on GAR-3 signaling. In *gar-3* deletion mutants, only 4.3% (n = 69) of the LCs reversed their orientation in response to 500 μM aldicarb (Fig. 2*D*), and higher concentrations of aldicarb did not change the outcome (1 mM aldicarb, 4.1% reversal, n = 24; 1.5 mM aldicarb, 0% reversal, n = 38). Conversely, in wild-type animals, when full-length GAR-3 fused to YFP (gar-3A::GAR-3::YFP, *syIs257*) was mildly overexpressed in the LC but not in the VNC, a much higher percentage of LCs (69.8% reversal, n = 86) reversed their orientation relative to LCs of animals with normal expression (28%, n = 64), all with aldicarb treatment (Fig. 2*D*). By blocking GAR-3 function in these GAR-3::YFP overexpressing animals with scopolamine, a *gar-3*-selective muscarinic receptor antagonist (22), none of the LCs responded to aldicarb treatment (0% reversal, n = 33) (Fig. 2*D*). GAR-3 is, therefore, required for LC reversal, and its activity determines LC response to ACh.

***gar-3* Functions in LC and Neurons.** In addition to *gar-3*'s function in the LC, *gar-3* plays a role in the cholinergic neurons to stimulate ACh release (13). To isolate the *gar-3* function in the LC from cholinergic neurons, we tissue-specifically restored *gar-3* expression to the LC in the *gar-3* mutant using sequences derived from the *nhr-67* promoter (23). LC expression of GAR-3::YFP in the *gar-3* mutant increased the percentage of LC reversals to 27.8% (n = 18) from 4.3% (n = 69) in the *gar-3* mutant alone (Fig. 2*E*). Cholinergic neuron-expressed GAR-3::YFP in *gar-3* mutants did not restore LC reversal (0% n = 9). These data suggest that *gar-3* function in the LC but not cholinergic neurons is necessary for regulating LC orientation. However, LCs expressing *gar-3* produced fewer reversals in the *gar-3* mutant background than in the wild-type background (27.8% vs. 69.8%), suggesting that *gar-3* expression in neurons also contributes to LC reversal. Expressing GAR-3::YFP in both the LC and the cholinergic neurons of the *gar-3* mutant completely restored the number of reversals (70.3%, n = 27) to that of wild-type animals with LC GAR-3::YFP overexpression (69.8%, n = 64). We conclude that *gar-3* contributes to two processes that result in LC reversal—increased ACh release by the cholinergic neurons and the LC's response to this increase in ACh.

We investigated whether cholinergic neurons are the source of ACh for LC reversal using two genes that are specifically expressed in cholinergic neurons. Mutants defective in ACh release produced little to no LC reversals in response to aldicarb, even in the sensitized GAR-3::YFP overexpression background. lf mutants of the ACh transporter *unc-17(lf)* had 8.3% reversal (n = 12), and mutants of choline acetyltransferase *cha-1(lf)* had 0% reversals (n = 12) in *gar-3::YFP* overexpressing animals (Fig. 2*F*).

***gar-3* Downstream Effectors Involved in Cell Reversal.** We next used this aldicarb assay to identify which of the known effectors of the *gar-3* G protein coupled receptor (GPCR) signaling pathway were being used by the LC. GAR-3 is known to activate Gαq/EGL-30, which then signals through two effectors, phospholipase C-β (PLCβ)/EGL-8 and TRIO/UNC-73 (11–13, 24–28). The mutants of these genes had fewer LC reversals in response to aldicarb even in the *gar-3::YFP* overexpression background (*egl-30* 2.6% reversals, n = 39; *egl-8* 0% reversals, n = 25; *unc-73* 12.5% reversals, n = 24; compared to wild-type 69.8% reversals, n = 86; all with *gar-3::YFP*) (Fig. 2*G*). This suggests that *gar-3* signaling utilizes both PLCβ and TRIO pathways downstream of Gαq activation for inducing LC reversal.

GAR-3 Receptor Relocalizes from Symmetric to Polarized in the Plasma Membrane. We observed GAR-3 expression in the LC using the *gar-3A* promoter, a 6 kb region upstream of the start of *gar-3* isoform a (12) to drive the expression of the full-length genomic GAR-3 tagged with a C-terminal YFP but not using the *gar-3B* promoter, a 3.5 kb sequence upstream of isoform b. GAR-3 localized to the LC plasma membrane as expected of the GPCR (Fig. 3 *A* and *B*). However, the distribution of GAR-3 within the membrane changes from one that is uniform in the L3 stage to one

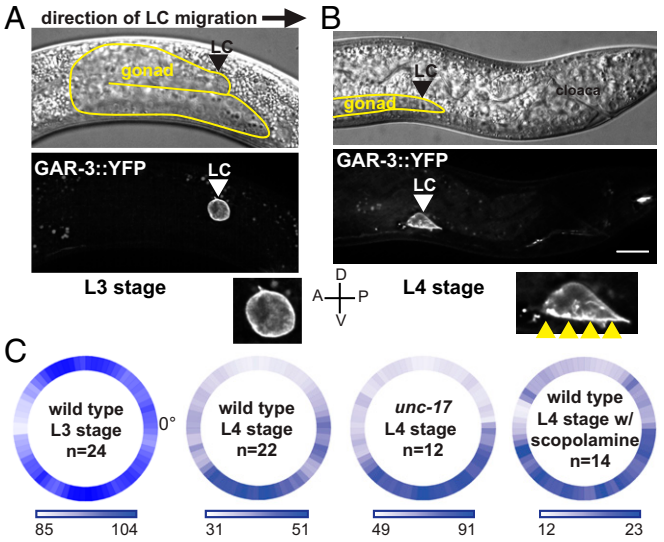

Fig. 3. GAR-3 changes from a uniform to an asymmetric membrane localization in the L4 stage. (*A* and *B*) Representative Nomarski and fluorescence images of animals expressing GAR-3::YFP in the L3 stage (*A*) and L4 stage (*B*). The gonad is outlined in yellow. Yellow arrowheads indicate GAR-3::YFP polarization on the ventral side of the L4 stage LC (*B*). (Scale bar is 10 μm.) (*C*) Radial plots of average GAR-3::YFP intensities in the LC plasma membrane of the wild-type L3 stage, wild-type L4 stage, *unc-17* mutant L4 stage, and scopolamine (muscarinic receptor antagonist)-treated wild-type L4 stage animals.

that is ventrally polarized and sometimes in puncta in the L4 stage (Fig. 3 *A* and *B* and *SI Appendix*, Fig. S3). This difference can be observed in the radial plot of average YFP intensities along the LC circumference in L3 (n = 24) and L4 (n = 22) stage males (Fig. 3*C* and *SI Appendix*, Table S1).

Because the GAR-3 receptor in the L4 stage is polarized toward the VNC, we investigated whether this redistribution depends on ACh signaling. We examined GAR-3::YFP localization in L4 stage animals with less cholinergic signaling by using a mutant of the ACh vesicular transporter *unc-17(lf)* and by treating a wild-type animal with a muscarinic receptor antagonist, scopolamine. While reducing GAR-3 activity affected the expression level of GAR-3, it did not change GAR-3′s ventrally polarized localization (Fig. 3*C*). This is consistent with previous findings in neurons that asymmetric GAR-3 localization is determined by its N-terminal interaction with the extracellular matrix on the ventral body wall rather than by receptor activity (13).

Discussion

We have investigated the in vivo function of the muscarinic ACh receptor in cell migration using the LC, an epithelial leader cell of gonad migration in *C. elegans*. We have identified two cell migration phenotypes associated with either increasing or decreasing ACh signaling that occurs through the muscarinic *gar-3* receptor during LC migration. The *gar-3* receptor lf resulted in subtle migratory path defects, such as overshooting a turn. The overactivation of the receptor with extra ACh resulted in the unexpected phenotype of the LC reversing its orientation that depended on the GAR-3 expression level. We also found that this reversal is activated through known *gar-3* effectors Gαq/EGL-30 and both phospholipase C-β (PLCβ)/EGL-8 and TRIO/UNC-73 pathways.

The low penetrance and subtlety of the defect for the *gar-3* lf mutant is likely due to ACh being one of many cues used by the LC for migration. Netrin and hemicentin are among the other known cues to play important roles in guiding and promoting LC migration (29–31), and their lf results in more obvious path defects. ACh is, therefore, not one of the main guidance cues but instead may be used to refine the course of migration. Mutants of ACh transporter *unc-17* and terminal cholinergic fate specifier *unc-3* also produced similar LC migration defects, suggesting that the *gar-3* receptor indeed uses ACh signaling for this function. *unc-3* mutants, however, produced higher rates of defects than either *gar-3* or *unc-17* mutants, which could be due to developmental defects in addition to reduced ACh signaling. Previous characterization of *unc-3* mutants have shown that not only do many motor neurons fail to take on their terminal cholinergic fates, but also the wiring of the neurons is abnormal (18). Also supporting this, when we disrupted *unc-3* function postembryonically using an inducible degron system, we did not observe LC migration defects seen with the null mutant, suggesting that developmental abnormalities in *unc-3* mutants contribute a major effect to LC migration defects.

The second phenotype associated with the role of GAR-3 is that it changes the orientation of the LC. When GAR-3 is overactivated by using aldicarb to block the breakdown of released ACh, the LC responded by reversing its orientation. While this complete reversal was caused by GAR-3 overactivation, normal levels of activation may modify LC orientation in more subtle ways. The GAR-3 receptors in the L4 stage LC are polarized toward the ventral plasma membrane, providing a way to relay spatial information for orienting the LC. In motor and ring inter neuron/motor neurons the localization and compartmentalization of GAR-3 to specific regions of the cell membrane have been shown to result in localized signaling that is crucial for its function (14, 32). GAR-3 localization may have a similar effect in the LC of activating subcellular regions and thereby creating a directionality. There is also a correlation between the GAR-3 receptor becoming polarized ventrally and the LCs reversal response to ACh signaling. The GAR-3 receptor redistributes from a uniform localization in the L3 stage to an asymmetric one only in the L4 stage at which point the LC becomes responsive to excess ACh stimulus. This overactivation phenotype suggests that even normal levels of *gar-3* activation may make smaller adjustments to LC orientation and thereby refine its migratory path.

A directionality to the GAR-3 signaling can come not only from the localization of the receptor, but also from the source of the signal, the cholinergic neurons along the LC's migratory path. While many non-neuronal cells produce ACh in mammals, in *C. elegans* the cholinergic neurons are the only known source of ACh based on the expression of genes required for ACh synthesis and release. Also, mutants of synaptic vesicle ACh transporter *unc-17*, which is expressed by cholinergic neurons or the cholinergic neuron terminal selector *unc-3* resulted in LC migration defects that were similar to *gar-3* deletion mutants. Since the cholinergic neurons reside in the VNC and their neurites extend to the DNC, the closest source of ACh for the LC at any point is either on its dorsal or ventral side, depending on its location along its migratory path. Additionally, there is a preanal cholinergic ganglion immediately posterior to the VNC (33) which potentially creates a higher gradient of ACh in the posterior end. This may explain why the LC reverses its orientation from posterior to anterior facing in response to excess ACh signaling only in this later stage of its migration. We do not know if this reversal indicates that normal levels of ACh act as a repulsive cue. There may be thresholds for various responses, and since the LC has other known guidance cues, it likely integrates several signals to determine a directionality.

The LC likely uses ACh that diffuses from the synaptic sites of cholinergic neurons as indicated by the involvement of *unc-17*, an acetylcholine vesicular transporter. EMs showed no evidence of synaptic contact, even though the LC approaches within several nanometers of VNC cell bodies and processes. This is consistent with our knowledge of worm anatomy that a basal lamina separates the gonad, including the LC, from the nerve cord (34). We

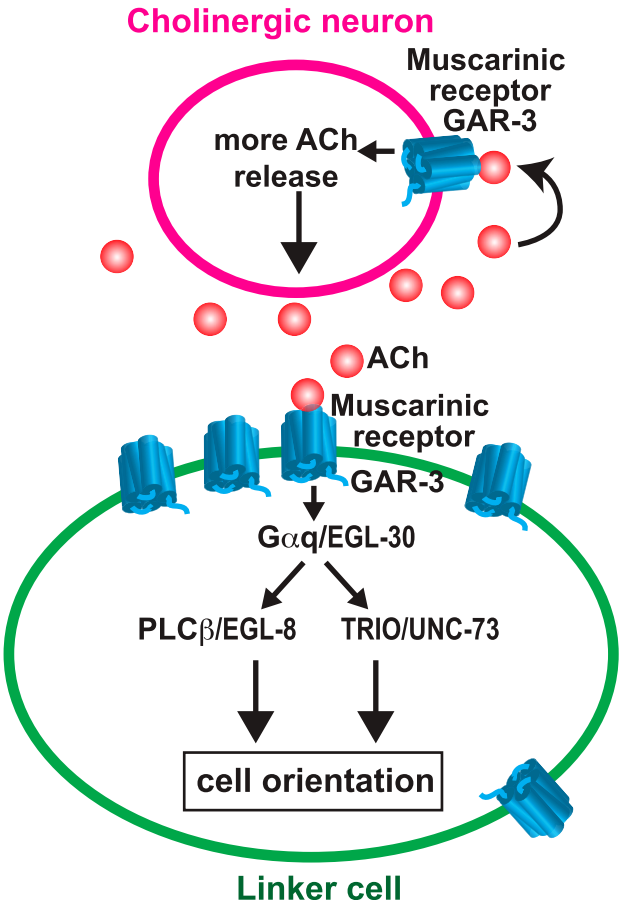

Fig. 4. Model for GAR-3 function in LC migration. The LC receives ACh signaling through the *gar-3* muscarinic receptor, which then signals through the Gαq subunit. Both PLCβ/*egl-8* and TRIO/*unc-73* pathways are used to affect the orientation of the LC. The LC function of GAR-3 depends on ACh signaling from the cholinergic neuron where GAR-3 promotes the release of ACh. In the L4 stage, GAR-3 localization is polarized toward the ventral side closer to the neurons releasing ACh. This likely causes asymmetric GAR-3 signaling in the L4 stage LC and may bias the LC to changing its orientation in response to ACh signaling.

hypothesize that synaptically released ACh diffuses across the basal lamina from cholinergic neurons to the LC and pseudocoelem. Although the path of diffusion from synaptic sites to the pseudocoelem is not clear, it was previously shown that ACh can travel long distances through the body, presumably through the pseudocoelem, to activate GAR-3 receptors at nonsynaptic sites (32). This mode of signaling has been shown for muscarinic receptors in mammals as well (35).

Based on our current investigation, our model for the role ACh signaling on this epithelial migration is that the LC receives ACh from nearby cholinergic neurons through extrasynaptic neurotransmission (Fig. 4). The ACh activates GAR-3 muscarinic receptors on the LC and signals through downstream effectors Gαq/EGL-30, phospholipase C-β (PLCβ)/EGL-8, and TRIO/UNC-73. As a result of this signal, the LC adjusts its orientation and, therefore, its direction of migration. Changes in LC orientation may, in part, be facilitated by the asymmetric localization of the GAR-3 receptor and ACh signal. Because M1/M3/M5 muscarinic receptor signaling is conserved with GAR-3 (10) and is used in mammalian cell migrations (1–4, 15, 16), further investigation may also reveal a conserved in vivo role for muscarinic receptors in various cell migrations.

Materials and Methods

***C. elegans* Strains.** *C. elegans* strains were cultured at room temperature using standard protocols unless indicated otherwise (36). Most animals used in this study were male and contained either *him-5(e1490)*V or, in the case that alleles of interest were on chromosome V, *him-8(e1489)* IV (37). A strain list can be found in the *SI Appendix*.

Generating the *unc-17β::gar-3::yfp::unc-54* Construct. The *unc-17β* promoter was PCR amplified using forward 5′AAGCTTTTGGTTTTCACAA TTTTCTGG3′ and reverse 5′ATTCCCCAACGAAGAGGACTGCATGGTTACT ATTTTGAACAAGAGATGCGG3′ primers off of plasmid KG65 (a gift from the Miller Laboratory). *gar-3::YFP::unc-54* was amplified off of PYL8 plasmid (12) using forward 5′ATGCAGTCCTCTTCGTTGGGGAAT3′ and reverse 5′AAGCTTTTGGTTTTCA CAATTTTCTGG- expand the long template PCR system (Roche). PCR fusion was performed using these two amplicons as a template and forward 5′AAGCTTTTGGTTTTCACAATTTTCTGG3′ and reverse 5′AAGCTTTTGGTTTTCACAATTTTCTGG primers.

Pharmacology Assays. Nematode growth media (NGM) plates containing 1 mM (–)-scopolamine hydrochloride (100 mM stock in ddH_20) and 1.5 mM levamisole (100 mM stock in ddH_20) were made by spreading stock solutions onto NGM plates. Plates containing 30 mM sodium azide (1 M stock in ddH_20) and 500 μM aldicarb (100 mM stock in 70% ethanol) were made by adding stock solutions into the NG media prior to pouring plates. All compounds are from Sigma-Aldrich.

LC reversal assays were conducted by placing either L3 or L4 stage males on 35 mm NGM plates containing chemicals for 2 h 15 min. The animals were then mounted on 2% agarose pads with 3 mM levamisole and examined on a Zeiss Axioscope equipped with a 100× objective and Nomarski optics. The LC morphology was scored as "reversed" only if the position of the nucleus was at the leading end of the cell.

EM. Samples were subjected to high-pressure freezing followed by freeze substitution processed for correlative fluorescence-EM analysis using a modified rapid approach that preserves native fluorescence (38–40). Briefly, following a modified fast freeze-substitution procedure with 0.1% UAc diluted in anhydrous acetone. Following the substitution procedure, samples were embedded in HM 20 acrylic resin mix. Samples were sectioned at 150 nm thickness and transferred to wafers using an array tomography protocol (38, 41). After drying, the wafers were imaged for fluorescence signal using a Zeiss fluorescent microscope equipped with 4′,6-diamidino-2-phenylindole and green fluorescent protein filters using ×20 and ×60 objectives. To analyze the ultrastructure, samples were contrasted with the UAc and lead citrate and observed using FEI Quanta 250 FEG scanning electron microscope (FEI, Eindhoven). Images were adjusted and superimposed using Photoshop (Adobe), ImageJ, and IMOD programs.

Image Analysis of LC GAR-3::YFP Localization. L3 or L4 stage males expressing *gar-3A::GAR-3::YFP* were mounted on 2% agarose pads with 3 mM levamisole. Z-stack images of LCs were taken on a Leica DMI 6000 microscope equipped with a 100× objective, Lumencor Spectra X illuminator, Andor camera, and MetaMorph software. Each z stack was deconvoluted using Huygens software (Scientific Volume Imaging) and converted into a "sum slices" z projection in Fiji.

Each projection image was then segmented to extract the cell body including its perimeter. We adopted two complementary approaches to segment cells: active contours based on the celebrated Chan–Vese model (42) and an adaptive mean threshold method. Results obtained with these methods were postprocessed using mathematical morphology operations to remove holes and dangling regions which were deemed too small when compared to expected cell size. Further manual editing was performed on a few cases to remove small protrusions captured during segmentation due to spurious signals. These protrusions represented, on average, 0.4% of the cell body for the L3 males (max = 0.6%, min = 0.2%) and 2.5% for the L4 males (max = 6.7%, min = 0.3%). Average values of *gar-3A::GAR-3::YFP* were collected on the perimeter of the cells to generate the relative concentration polar plots shown in Fig. 3. For every pixel on the boundary of the cell we determined its polar angle with respect to the centroid of the cell mask and its neighborhood intensity computed as the average signal in a disk of radius 5 centered at the pixel. The tint in each arc of 5° in a radial plot is proportional to the mean neighborhood intensity of all boundary pixels whose polar angles are within the arc interval. See *SI Appendix*, Fig. S4 for macros.

Data Availability. All study data are included in the article and supporting information.

ACKNOWLEDGMENTS. We thank laboratory members, particularly Pei Yin Shih, Ravi Nath, and Han Wang, for comments on the paper. Some strains were provided by the *Caenorhabditis* Genetics Center, which is funded by NIH Office of Research Infrastructure Programs (grant P40 OD010440), and by the *C. elegans* Gene Knockout Project at the Oklahoma Medical Research Foundation, which was part of the International *C. elegans* Gene Knockout Consortium. For image collection and analysis, we used the Caltech Biological Imaging Facility and the Center for Advanced Methods in Biological Image Analysis. We received microscopy training from Dr. Andres Collazo and Huygens software training from Say-Tar Goh. Dr. Rene Garcia, Dr. Derek Sieburth, and Dr. Kenneth Miller kindly provided strains and reagents. This work was supported by HHMI with whom P.W.S. was an investigator and by US Public Health Service NIH, *Eunice Kennedy Shriver* Institute of Child Health and Human Development grant R01 HD091327 to P.W.S. and M.K.

1. S. Li *et al*., Nicotinic acetylcholine receptor alpha7 subunit mediates migration of vascular smooth muscle cells toward nicotine. *J. Pharmacol. Sci.* **94**, 334–338 (2004).
2. A. I. Chernyavsky, J. Arredondo, J. Wess, E. Karlsson, S. A. Grando, Novel signaling pathways mediating reciprocal control of keratinocyte migration and wound epithelialization through M3 and M4 muscarinic receptors. *J. Cell Biol.* **166**, 261–272 (2004).
3. J. M. Tang *et al*., Acetylcholine induces mesenchymal stem cell migration via Ca2+/PKC/ERK1/2 signal pathway. *J. Cell. Biochem.* **113**, 2704–2713 (2012).
4. R. R. Resende, A. Adhikari, Cholinergic receptor pathways involved in apoptosis, cell proliferation and neuronal differentiation. *Cell Commun. Signal.* **7**, 20 (2009).
5. M. Amit, S. Na'ara, Z. Gil, Mechanisms of cancer dissemination along nerves. *Nat. Rev. Cancer* **16**, 399–408 (2016).
6. S. Zhang *et al*., Distinct roles of cholinergic receptors in small cell lung cancer cells. *Anticancer Res.* **30**, 97–106 (2010).
7. E. A. Parnell, I. E. Calleja-Macias, M. Kalantari, S. A. Grando, H. U. Bernard, Muscarinic cholinergic signaling in cervical cancer cells affects cell motility via ERK1/2 signaling. *Life Sci.* **91**, 1093–1098 (2012).
8. U. Theisen, C. Hennig, T. Ring, R. Schnabel, R. W. Köster, Neurotransmitter-mediated activity spatially controls neuronal migration in the zebrafish cerebellum. *PLoS Biol.* **16**, e2002226 (2018).
9. E. M. Schwarz, M. Kato, P. W. Sternberg, Functional transcriptomics of a migrating cell in *Caenorhabditis elegans*. *Proc. Natl. Acad. Sci. U.S.A.* **109**, 16246–16251 (2012).
10. R. M. Eglen, Muscarinic receptor subtypes in neuronal and non-neuronal cholinergic function. *Auton. Autacoid Pharmacol.* **26**, 219–233 (2006).
11. K. A. Steger, L. Avery, The GAR-3 muscarinic receptor cooperates with calcium signals to regulate muscle contraction in the *Caenorhabditis elegans* pharynx. *Genetics* **167**, 633–643 (2004).
12. Y. Liu, B. LeBoeuf, L. R. Garcia, G alpha(q)-coupled muscarinic acetylcholine receptors enhance nicotinic acetylcholine receptor signaling in *Caenorhabditis elegans* mating behavior. *J. Neurosci.* **27**, 1411–1421 (2007).
13. J. P. Chan, Z. Hu, D. Sieburth, Recruitment of sphingosine kinase to presynaptic terminals by a conserved muscarinic signaling pathway promotes neurotransmitter release. *Genes Dev.* **26**, 1070–1085 (2012).
14. M. Hendricks, H. Ha, N. Maffey, Y. Zhang, Compartmentalized calcium dynamics in a *C. elegans* interneuron encode head movement. *Nature* **487**, 99–103 (2012).
15. A. Belo *et al*., Muscarinic receptor agonists stimulate human colon cancer cell migration and invasion. *Am. J. Physiol. Gastrointest. Liver Physiol.* **300**, G749–G760 (2011).
16. G. Lin, L. Sun, R. Wang, Y. Guo, C. Xie, Overexpression of muscarinic receptor 3 promotes metastasis and predicts poor prognosis in non-small-cell lung cancer. *J. Thorac. Oncol.* **9**, 170–178 (2014).
17. B. Prasad, O. Karakuzu, R. R. Reed, S. Cameron, *unc-3*-dependent repression of specific motor neuron fates in *Caenorhabditis elegans*. *Dev. Biol.* **323**, 207–215 (2008).
18. P. Kratsios, A. Stolfi, M. Levine, O. Hobert, Coordinated regulation of cholinergic motor neuron traits through a conserved terminal selector gene. *Nat. Neurosci.* **15**, 205–214 (2011).
19. A. Alfonso, K. Grundahl, J. S. Duerr, H. P. Han, J. B. Rand, The *Caenorhabditis elegans unc-17* gene: A putative vesicular acetylcholine transporter. *Science* **261**, 617–619 (1993).
20. L. Zhang, J. D. Ward, Z. Cheng, A. F. Dernburg, The auxin-inducible degradation (AID) system enables versatile conditional protein depletion in *C. elegans*. *Development* **142**, 4374–4384 (2015).
21. T. Patel, O. Hobert, Coordinated control of terminal differentiation and restriction of cellular plasticity. *eLife* **6**, e24100 (2017).
22. Y. S. Lee *et al*., Characterization of GAR-2, a novel G protein-linked acetylcholine receptor from *Caenorhabditis elegans*. *J. Neurochem.* **75**, 1800–1809 (2000).
23. J. A. Malin, M. J. Kinet, M. C. Abraham, E. S. Blum, S. Shaham, Transcriptional control of non-apoptotic developmental cell death in *C. elegans*. *Cell Death Differ.* **23**, 1985–1994 (2016).
24. B. Perez-Mansilla, S. Nurrish, A network of G-protein signaling pathways control neuronal activity in *C. elegans*. *Adv. Genet.* **65**, 145–192 (2009).
25. L. Brundage *et al*., Mutations in a C. elegans Gqalpha gene disrupt movement, egg laying, and viability. *Neuron* **16**, 999–1009 (1996).
26. K. G. Miller, M. D. Emerson, J. B. Rand, Goalpha and diacylglycerol kinase negatively regulate the Gqalpha pathway in *C. elegans*. *Neuron* **24**, 323–333 (1999).
27. J. B. Rand, R. L. Russell, Choline acetyltransferase-deficient mutants of the nematode *Caenorhabditis elegans*. *Genetics* **106**, 227–248 (1984).
28. S. L. Williams *et al*., Trio's Rho-specific GEF domain is the missing Galpha q effector in *C. elegans*. *Genes Dev.* **21**, 2731–2746 (2007).
29. M. Su *et al*., Regulation of the UNC-5 netrin receptor initiates the first reorientation of migrating distal tip cells in *Caenorhabditis elegans*. *Development* **127**, 585–594 (2000).
30. B. E. Vogel, E. M. Hedgecock, Hemicentin, a conserved extracellular member of the immunoglobulin superfamily, organizes epithelial and other cell attachments into oriented line-shaped junctions. *Development* **128**, 883–894 (2001).
31. M. Kato, P. W. Sternberg, The *C. elegans* tailless/Tlx homolog *nhr-67* regulates a stage-specific program of linker cell migration in male gonadogenesis. *Development* **136**, 3907–3915 (2009).
32. J. P. Chan *et al*., Extrasynaptic muscarinic acetylcholine receptors on neuronal cell bodies regulate presynaptic function in *Caenorhabditis elegans*. *J. Neurosci.* **33**, 14146–14159 (2013).
33. E. Serrano-Saiz *et al*., A neurotransmitter Atlas of the *Caenorhabditis elegans* male nervous system reveals sexually dimorphic neurotransmitter usage. *Genetics* **206**, 1251–1269 (2017).
34. J. M. Kramer, Basement membranes. *WormBook*, 10.1895/wormbook.1.16.1 (2005).
35. M. Sarter, V. Parikh, W. M. Howe, Phasic acetylcholine release and the volume transmission hypothesis: Time to move on. *Nat. Rev. Neurosci.* **10**, 383–390 (2009).
36. S. Brenner, The genetics of *Caenorhabditis elegans*. *Genetics* **77**, 71–94 (1974).
37. H. R. Horvitz, S. Brenner, J. Hodgkin, R. K. Herman, A uniform genetic nomenclature for the nematode *Caenorhabditis elegans*. *Mol. Gen. Genet.* **175**, 129–133 (1979).
38. I. Kolotuev, Positional correlative anatomy of invertebrate model organisms increases efficiency of TEM data production. *Microsc. Microanal.* **20**, 1392–1403 (2014).
39. I. Kolotuev, Y. Schwab, M. Labouesse, A precise and rapid mapping protocol for correlative light and electron microscopy of small invertebrate organisms. *Biol. Cell* **102**, 121–132 (2009).
40. A. Burel *et al*., A targeted 3D EM and correlative microscopy method using SEM array tomography. *Development* **145**, dev160879 (2018).
41. K. D. Micheva, S. J. Smith, Array tomography: A new tool for imaging the molecular architecture and ultrastructure of neural circuits. *Neuron* **55**, 25–36 (2007).
42. A. L. Cunha, A. H. Roeder, E. M. Meyerowitz, Segmenting the sepal and shoot apical meristem of Arabidopsis thaliana. *Annu. Int. Conf. IEEE Eng. Med. Biol. Soc.* **2010**, 5338–5342 (2010).